Journal of Pharmacological and Toxicological Methods 106 (2020) 106936

Contents lists available at ScienceDirect

Journal of Pharmacological and Toxicological Methods

journal homepage: www.elsevier.com/locate/jpharmtox

FLA

Use of computed tomography to assess subcutaneous drug dispersion with recombinant human hyaluronidase PH20 in a swine model

Robert J. Connor [a], Darin M. Taverna [a], Karla Thrall [b], Michael J. LaBarre [c], David W. Kang [c,*]

[a] Formerly of Halozyme Therapeutics, Inc., San Diego, CA, USA
[b] Formerly of SNBL USA Ltd., Everett, Washington, USA
[c] Halozyme Therapeutics Inc., San Diego, CA, USA

ARTICLE INFO

Keywords:
(1−10): computed tomography
CT
Drug dispersion
Hyaluronan
Methods
Non-invasive imaging methods
Recombinant human hyaluronidase PH20
rHuPH20
Subcutaneous drug delivery
Swine model

ABSTRACT

Introduction: Subcutaneous (SC) formulations of therapeutics with recombinant human hyaluronidase PH20 (rHuPH20) are currently approved across various disease indications. The rHuPH20-mediated enzymatic degradation of SC hyaluronan (HA) facilitates bulk fluid flow and dispersion of co-administered therapeutics. However, current methods of quantifying dispersion in the SC space are limited. Here, a novel method is outlined to quantify and follow rapid SC volumetric dispersion of a representative therapeutic fluid in the presence of rHuPH20 using computed tomography (CT).

Methods: Ten Yucatan miniature swine were randomized to three groups. Animals received simultaneous infusions of contrast agent (CA) alone (left side of the animal) or in combination with rHuPH20 (right side) at infusion rates of 2.5, 5, or 10 mL/min. Spiral CT scans (1.5 mm thickness) were conducted before and after the infusion and at regular time intervals throughout. Scans were used to create three-dimensional (3D) reconstructions of the fluid pockets and analyze surface area, volume, and sphericity.

Results: 3D reconstruction showed increased dispersion of CA with rHuPH20 compared with CA alone, with fenestration and increased dispersion in the craniocaudal and lateromedial directions. The CA with rHuPH20 fluid pockets showed an average increase of 46% in surface area ($p = 0.001$), a 35% increase in volume ($p = 0.001$) and a 17% decrease in sphericity post-infusion compared with CA alone at 30 min post-infusion.

Discussion: This exploratory study confirms the value of CT imaging as a non-invasive method of assessing real-time spatial and temporal behavior of SC-administered fluids. This technique could help to assess the dispersion pattern of novel rHuPH20 SC co-formulations.

1. Introduction

The subcutaneous (SC) delivery of therapeutics is becoming increasingly common across multiple disease areas including oncology, rheumatoid arthritis, multiple sclerosis, and primary immunodeficiency. When available, the SC route of administration is generally preferred by both healthcare providers and patients over intravenous (IV) infusion, owing to its less invasive nature, improved tolerability, increased convenience for patients, and reduced healthcare administration time, costs, and resource use (Awwad & Angkawinitwong, 2018; Bittner, Richter, Hourcade-Potelleret, Herting, & Schmidt, 2014; Bittner, Richter, & Schmidt, 2018; De Cock et al., 2016; Pivot et al., 2014; Richter & Jacobsen, 2014; Williams & Edwards, 2006; Wynne et al., 2013). However, standard SC delivery systems are associated with volume limitations, with 2 mL generally considered the upper limit for rapid delivery in a single infusion (Hunter, 2008; Richter & Jacobsen, 2014), whereas the clinical therapeutic dose of many therapeutics requires administration of a volume in excess of 2 mL (Roche Roche, 2017; Takeda Pharmaceuticals, 2014). Standard SC delivery of large volumes of therapeutics can result in side effects including local pain and irritation, tissue distortion, and induration at infusion sites, causing discomfort and decreasing patient compliance for repeat infusions (Bittner, Richter, & Schmidt, 2018; Bookbinder et al., 2006; Hunter, 2008). The alternative of fractionating large SC volumes into multiple doses or delivery sites is more time-consuming, inconvenient for both the patient and healthcare provider, can be more painful for the patient, and can reduce the reproducibility of therapeutic serum levels at different administrations (Bittner, Richter, & Schmidt, 2018).

* Corresponding author at: Halozyme Therapeutics Inc., 11388 Sorrento Valley Rd, San Diego, CA, USA
E-mail address: publications@halozyme.com (D.W. Kang).

https://doi.org/10.1016/j.vascn.2020.106936
Received 6 December 2019; Received in revised form 15 July 2020; Accepted 22 September 2020
Available online 22 October 2020

Hyaluronan (HA), a naturally occurring glycosaminoglycan, is one of the main components of the extracellular matrix in SC connective tissue and plays an important role in limiting SC drug delivery. HA forms a "gel-like" substance with water, reducing the movement of fluids in the SC space and creating a barrier to fluid flow (Frost, 2007). HA is synthesized by hyaluronan synthases and degraded by hyaluronidase enzymes as part of normal physiological processes, with approximately one third of the total HA content in the body turned over every 24 h (Jadin, Bookbinder, & Frost, 2012; Stern, 2003; Vigetti, Viola, Karousou, Luca, & Passi, 2014). Animal-derived hyaluronidases have a long history of use to improve the dispersion and absorption of subcutaneously administered therapeutics (Atkinson, 1949; Watson, 1993).

Recombinant human hyaluronidase PH20 (rHuPH20) is a highly purified recombinant human form of the PH20 enzyme comprising human, rather than animal, amino acid sequences to minimize the risk of allergenicity associated with the animal preparations (Baumgartner, Gomar-Hoss, Sakr, Ulsperger, & Wogritsch, 1998; Locke, Maneval, & LaBarre, 2019; Yocum, Kennard, & Heiner, 2007). The action of rHuPH20 in the SC space has been shown to be local and transient, with degradation of HA resulting in a temporary reduction of the resistance to fluid flow (Bookbinder et al., 2006; Frost, 2007). The degradation of SC HA thus currently allows administration of up to 600 mL, and theoretically greater volumes, per infusion in a single site, enabling the increased dispersion and absorption of subcutaneously administered therapeutics (Bookbinder et al., 2006; Vaughn & Muchmore, 2011; Wasserman, 2012; Takeda Pharmaceuticals, 2014) (Fig. 1), while minimizing potential disadvantages of SC delivery.

A focused biodistribution study in NCr nu/nu mice injected with rHuPH20 confirmed that rHuPH20 has a short half-life of 13–20 min in the skin (Kang, et al. Unpublished results). In agreement with these results, dye dispersion studies found that rHuPH20 delivered at one site did not impact dye dispersion at a distal skin site (Kang, et al. Unpublished results). In addition, no meaningful rHuPH20 activity was observed in lymph tissue or in plasma, suggesting that rHuPH20 is not transported in meaningful quantities outside the SC tissues (Kang, et al. Unpublished results). Currently, rHuPH20 is applied as part of six commercially available products. Hylenex® recombinant (Halozyme Therapeutics, Inc., San Diego, CA), a hyaluronidase human injection (rHuPH20 alone; available in the US), is used as a tissue permeability modifier (Halozyme Therapeutics, Inc, 2016). The other five products (available in the EU/US) are: HyQvia®/HYQVIA® (IgG with hyaluronidase; Takeda Pharmaceuticals, Tokyo, Japan), for the treatment of primary immunodeficiency (Baxalta Innovation GmbH, 2018; Takeda Pharmaceuticals, 2014); Herceptin® SC/HERCEPTIN HYLECTA™ (trastuzumab with hyaluronidase; Roche Products Ltd., Basel, Switzerland), for the treatment of HER2+ breast cancer (Roche Registration GmbH, 2018a, 2018b); PHESGO® (US only; pertuzumab, trastuzumab, and hyaluronidase; Genentech Inc., South San Francisco, California, USA), for the treatment of HER2+ breast cancer (Genentech Inc, 2020); MabThera® SC/RITUXAN HYCELA® (rituximab with hyaluronidase; Roche, Basel, Switzerland), for the treatment of chronic lymphocytic leukemia and some subtypes of non-Hodgkin's lymphoma (Biogen and Genentech USA Inc, 2017; Roche Registration GmbH, 2018a, 2018b), and DARZALEX FASPRO™/DARZALEX® SC (daratumumab with hyaluronidase; Janssen Biotech, Horsham, Pennsylvania, USA), for the treatment of multiple myeloma (Genmab, 2020; Janssen Biotech Inc, 2020). Several other approved therapeutics and investigational products in the areas of hematology and immuno-oncology are also in clinical development with rHuPH20 (Locke, Maneval, & LaBarre, 2019).

As rHuPH20 is being applied to a range of co-administered therapeutics, there is an increasing interest in quantifying its effect on fluid dispersion in the SC space to further understand the mechanics of rHuPH20-mediated fluid dispersion and improve the development of future SC formulations of therapeutics. In this exploratory study, we sought to use computed tomography (CT) to quantitatively measure the SC volumetric dispersion of a representative therapeutic fluid with and without rHuPH20. This methodology allows characterization of spatial drug distribution in three dimensions (3D) following SC infusion of co-administered therapeutics (Thomsen et al., 2012). The study was conducted in a swine model, which is considered representative of the human SC space (Richter & Jacobsen, 2014).

2. Methods

2.1. Ethics

This study was approved by SNBL USA Ltd. Institutional Animal Care and Use Committee and was carried out in compliance with the National Institutes of Health guide for care and use of laboratory animals (National Research Council, 2011).

2.2. Animals and materials

The study used 10 female, purpose-bred, naïve Yucatan miniature swine (*Sus scrofa domestica*). Animals were litter matched, aged between 3 and 4 months and were acclimated to the study room for a minimum of 5 days before receiving SC infusions. Body weights of the animals ranged from 12.1 to 18.3 kg on the day of dosing (Day 1).

For the purposes of the study, the contrast agent iodixanol (Visipaque; GE Healthcare, Inc., Marlborough, MA) was used as a surrogate representative therapeutic fluid. The solution used (hereafter referred to as contrast agent [CA]) contained 550 mg/mL iodixanol, equivalent to 270 mg/mL iodine along with 0.074 mg/mL calcium chloride dihydrate and 1.87 mg/mL sodium chloride, to create an isotonic solution for injection (GE Healthcare Inc, 1996). The solutions investigated in the study were CA alone, or CA co-mixed with rHuPH20 at a final concentration of 2000 U/mL, for a total infusion volume of 10 mL.

The dispersion of CA was monitored by sequential CT scanning using a SOMOTOM® CT Scope (Siemens Healthcare GmbH, Erlangen, Germany). The scanning parameters used were as follows: spiral CT scan with slice thickness of 1.5 mm, 110 kV potential, 100 mAs, 1.0 s rotation time, 1.05 pitch level, and B31s medium smooth plus kernel.

2.3. Study design

The ten animals were randomized to three study groups in a weight-stratified manner to ensure average body weights were comparable between groups. The number of animals per group was selected to properly characterize responses related to rHuPH20 at different infusion rates. Three animals received infusions at 2.5 mL/min, three animals received infusions at 5 mL/min and four animals received infusions at 10 mL/min, while maintaining the same total volume of infusion.

On Day 1, the animals were anesthetized using an intramuscular injection of Telazol® (tiletamine hydrochloride and zolazepam hydrochloride) and maintained on isoflurane gas for the duration of the infusion. Once anesthetized, the animals were placed on the CT scanner in dorsal recumbence and were immobilized with the head pointing away from the scanner gantry. Each animal received two simultaneous 10 mL SC infusions of CA, either alone (left side of the animal) or in combination with rHuPH20 (right side of the animal), at either 2.5, 5, or 10 mL/min depending on the treatment group (Table 1). Infusion needles (23G) were inserted subcutaneously on the lower abdominal region (Fig. 2).

Spiral CT scans with slice thickness of 1.5 mm were conducted before the initiation of dosing and at the specified time intervals during and after infusion (Table 1). The volume and surface area of CA in the SC space were measured at each imaging timepoint. Images were obtained throughout the infusion and at 1, 2, 4, 6, 8, 10, 12 (except for one animal in the 2.5 mL/min treatment group), 15, 17, 20, 25, and 30 min post-infusion. Upon completion of the CT scans the animals were euthanized by an overdose of euthanasia solution while still under anesthesia.

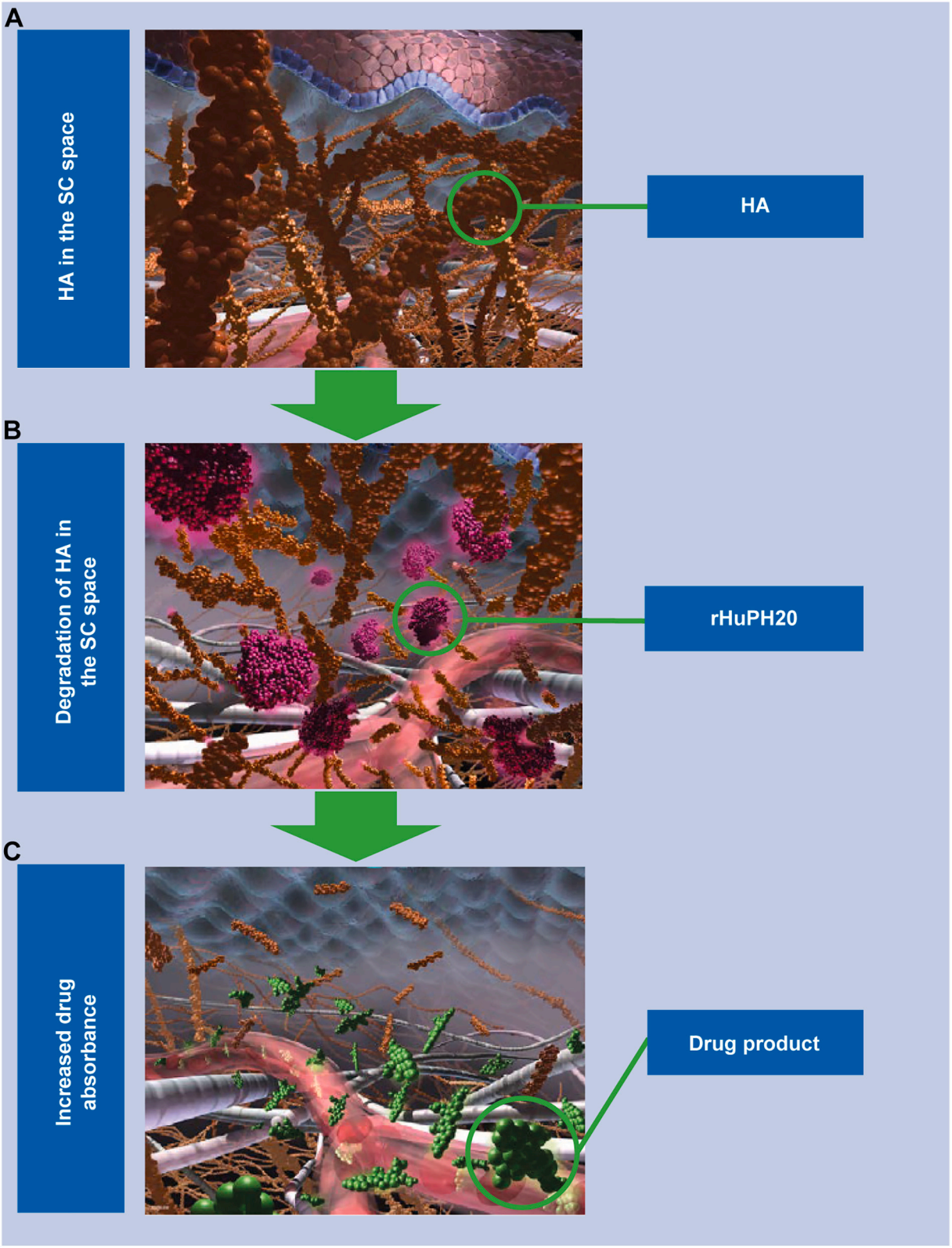

Fig. 1. rHuPH20 mechanism of action. (A) HA is a naturally occurring glycosaminoglycan present in the extracellular matrix of the SC space; (B) degradation of HA by rHuPH20 can reduce resistance to bulk fluid flow and; (C) enhance permeation of co-administered therapeutics.
HA, hyaluronan; rHuPH20, recombinant human hyaluronidase PH20; SC, subcutaneous.

Table 1
Summary of (A) study groups and imaging timepoints, and (B) statistics at 30 min post-infusion.

(A)

Group	Infusion flow rate (mL/min)	CT scan imaging timepoint during infusion (sec)	CT scan imaging timepoint post-infusion (min)
1	2.5	Pre, 24, 48, 72, 96, 120, 144, 168, 192, 216, 240	1, 2, 4, 6, 8, 10, 15, 17, 20, 25, 30
2	5	Pre, 12, 24, 36, 48, 60, 72, 84, 96, 108, 120	1, 2, 4, 6, 8, 10, 12, 15, 17, 20, 25, 30
3	10	Pre, 12, 24, 36, 48, 60	1, 2, 4, 6, 8, 10, 12, 15, 17, 20, 25, 30

(B)

	Infusion flow rate (mL/min)	*n*	CA Alone		CA + rHuPh20		Difference (%)	Statistical test	95% CI (range)	*p*-value
			Mean	SD	Mean	SD				
Surface Area	all	10	6778 mm^2	431	9911 mm^2	678	46	unpaired *t*-test	38–54%	< 0.0001
Volume	all	10	27,175 mm^3	2127	36,609 mm^3	2435	35	unpaired *t*-test	27–43%	< 0.0001
Sphericity	all	10	0.646	0.040	0.539	0.023	−17	unpaired *t*-test	−12 to −21%	< 0.0001

CT, computed tomography.
95% CI, 95% confidence interval; CA, contrast agent; rHuPH20, recombinant human hyaluronidase PH20.

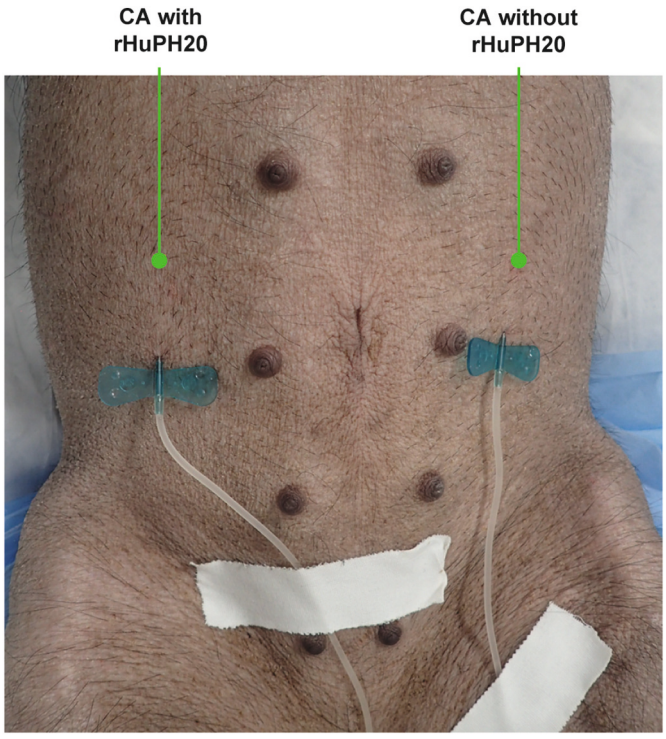

Fig. 2. Location of SC infusions of the CA either alone (left side of the Yucatan miniature swine) or in combination with rHuPH20 (right side of the Yucatan miniature swine), using an animal from the 2.5 mL/min flow rate group as an example.
SC, subcutaneous; CA, contrast agent; rHuPH20, recombinant human hyaluronidase PH20.

2.4. 3D reconstructions

A series of 3D representative reconstructions were prepared from scans of the animals at four post-infusion timepoints (0, 10, 20, and 30 min) to compare the changing sizes and shapes of the fluid pockets over time. The lower threshold used for the analysis of the CT data was 180 Hounsfield units (HU) and the upper threshold was 4000 HU. The lower threshold was chosen to capture the surface of the CA at a concentration that allowed it to be distinct from the surrounding tissue; the upper threshold of 4000 HU represents a value in excess of the densest tissue and was a necessary parameter to capture the fluid pocket as a region of interest (ROI). ROIs were captured using Horos software (Nimble Co LLC, Annanapolis, MD).

2.5. Image analyses and calculations

A veterinary imaging consultant (Veterinary Imaging Center of San Diego, San Diego, CA) provided evaluation and calculation of the dispersion of the CA with and without rHuPH20 over time. Volumes and surface areas were calculated as a function of time and rHuPH20 status (presence or absence), using Blender® software version 2.79 (Blender Foundation, Amsterdam, Netherlands). Data were recorded and analyzed using Microsoft Excel® (Microsoft Corporation, Redmond, WA) and statistical analyses were carried out using Prism version 7 (GraphPad, San Diego, CA). Unpaired *t*-tests were used for analyses of surface area, volume, and sphericity.

To assess the overall shapes of the post-infusion fluid pockets, the sphericity of the pockets was evaluated. Sphericity is a measure of how closely the shape of an object approaches that of a mathematical sphere, ranging from 0 (non-spherical) to 1.0 (completely spherical). This unitless metric allows for a mathematical description of the dispersion patterns of a representative therapeutic fluid over time. Sphericity was determined at each timepoint using the following formula (Wadell, 1935):

$$Sphericity = \Psi = \frac{(36\pi)^{\frac{1}{3}} V_C^{\frac{2}{3}}}{A_C}$$

where V_C = Volume of CA; A_C = Surface area of CA; and it is assumed the CA objects are simply connected domains with no holes.

3. Results

3.1. Dispersion of CA with and without rHuPH20

Administration of the CA with rHuPH20 resulted in minimal post-infusion swelling, with a fluid pocket that was considerably flatter and wider compared with administering CA alone (Fig. 3A). Analyses of post-infusion dispersion based on 3D reconstruction (with animal torso included) showed that the peripheral contour of rHuPH20-facilitated CA was highly fenestrated, dispersing in the craniocaudal and lateromedial directions. In comparison, the infusion of CA alone was relatively

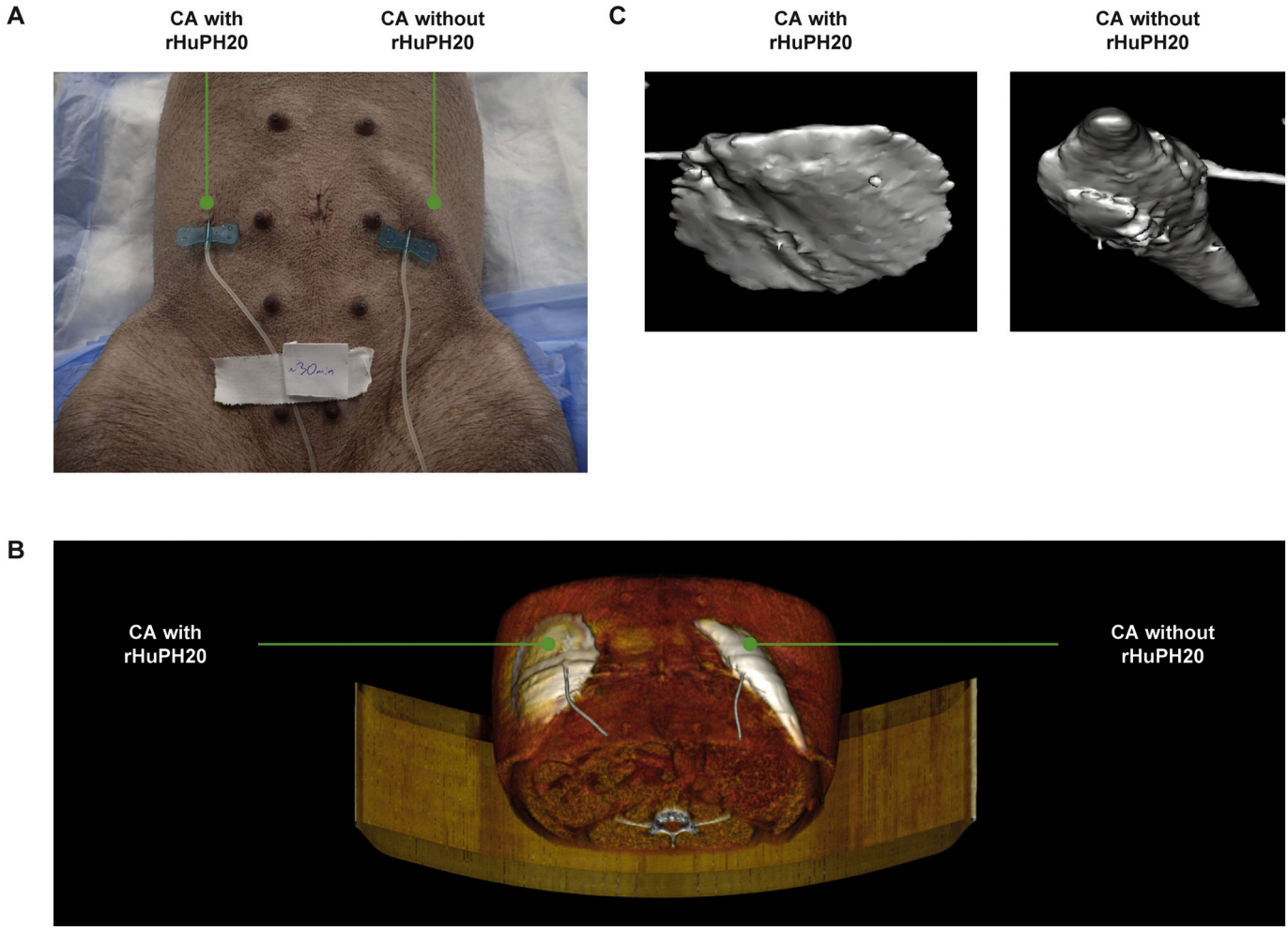

Fig. 3. Dispersion of a CA being subcutaneously infused with and without rHuPH20. (A) Administration of the CA with rHuPH20 resulted in minimal post-infusion swelling compared with administration of the CA alone; (B) 3D reconstruction of CA dispersion with the density threshold adjusted to include the structure of the animal surfaces; (C) 3D reconstruction of CA dispersion at 30 min post-infusion, with the density threshold adjusted to visualize only the infusion set, fluid pockets, and bone for reference using an animal from the 2.5 mL/min flow rate group as an example.
3D, 3-dimensional; CA, contrast agent; rHuPH20, recombinant human hyaluronidase PH20.

unchanged, with a well-defined peripheral margin (Fig. 3B). Increasing the density threshold used for image analyses allowed reconstruction of CA dispersion with and without rHuPH20, while demonstrating the fluid pocket's spatial relationship to the high-density animal skeleton (Fig. 3C).

3.2. Changes in the volume and surface area of the fluid pockets over time

The volume and surface area of rHuPH20-facilitated infusions increased throughout the post-infusion period (monitored for up to 30 min after infusion), while the volume and surface area of CA alone showed only minor increases during this time period (Fig. 4). At the 30-min post-infusion timepoint, averaged across infusion rates, rHuPH20-facilitated infusions showed a significant 46% increase in surface area and a significant 35% increase in volume compared with CA alone (surface area: unpaired *t*-test, $p < 0.0001$, 95% CI: 38–54%; volume: unpaired t-test; $p < 0.0001$, 95% CI: 27–43%) averaged across infusion rates (Table 1B).

3.3. Changes in length, width, and height of the fluid pockets over time

Compared with infusions of CA alone, infusions of CA combined with rHuPH20 showed enhanced dispersion across craniocaudal (length; Fig. 5A) and lateromedial (width; Fig. 5B) dimensions, accompanied by greater decreases in height (Fig. 5C) of the fluid pockets over time. The lengths and widths of the fluid pockets continued to increase throughout the post-infusion period for rHuPH20-facilitated infusions of CA, while infusions of CA alone showed only minor increases in these dimensions (Fig. 5A and B). Meanwhile, the heights of the fluid pockets were found to decrease much more rapidly for infusions of CA with rHuPH20 than for infusions of CA alone (Fig. 5C). Increasing the infusion rate from 2.5 mL/min to 5 mL/min or 10 mL/min did not result in changes in width or height of the fluid pockets for CA alone or with rHuPH20, during or post-infusion.

3.4. Sphericity of post-infusion fluid pockets for CA with and without rHuPH20

Infusions of CA with rHuPH20 showed a continuous decrease in sphericity post-infusion, while the sphericity of the infusion pockets of CA administered alone remained relatively unchanged over the post-infusion period (Fig. 6). At the 30-min post infusion timepoint, rHuPH20-facilitated infusions showed a significant 17% decrease in sphericity compared with CA alone, averaged across infusion rates (unpaired *t*-test, $p < 0.0001$, 95% CI: 12–21%; Table 1B).

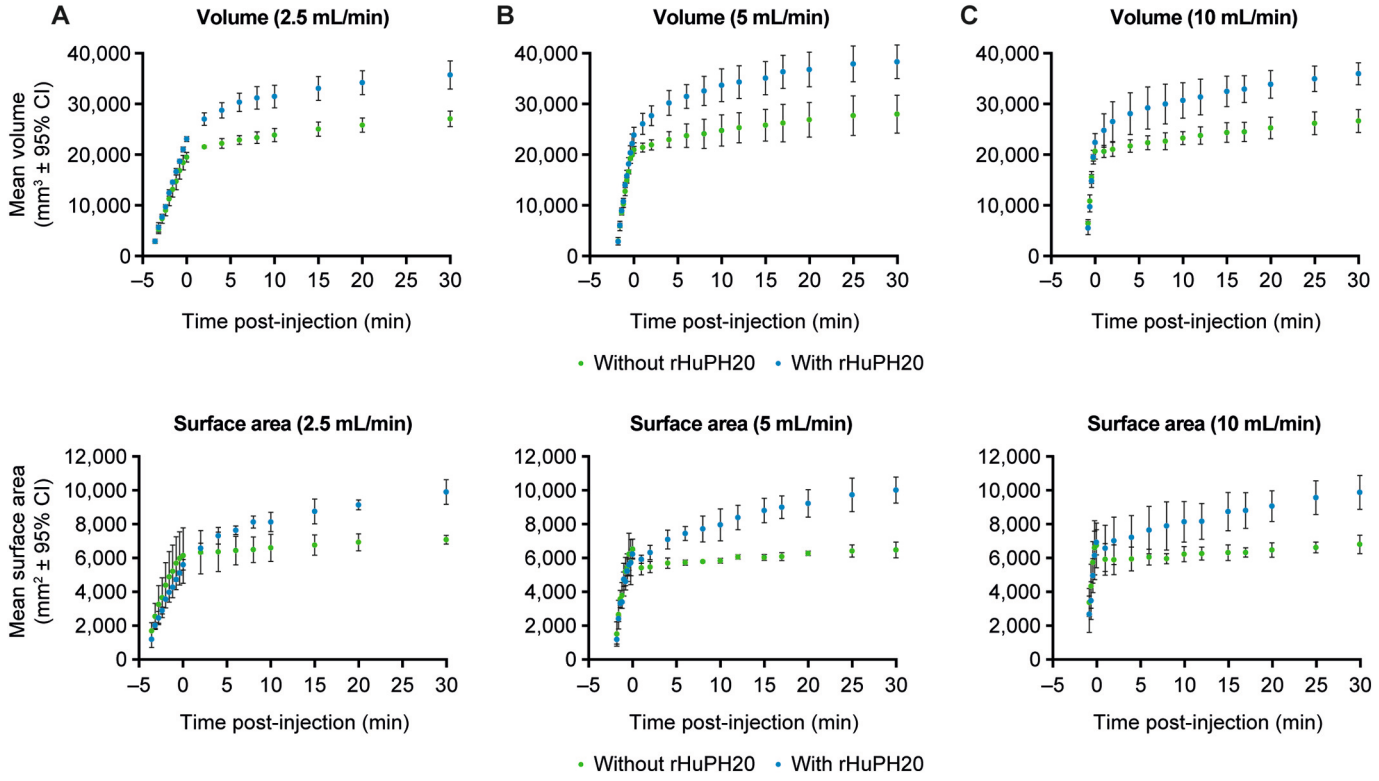

Fig. 4. Comparison of SC fluid pocket volumes and surface areas of CA with and without rHuPH20 (10 mL) over time for different infusion rates. (A) 2.5 mL/min; (B) 5 mL/min; (C) 10 mL/min. The averages (mean) of each infusion rate group ±95% CI are reported.
95% CI, 95% confidence interval; CA, contrast agent; rHuPH20, recombinant human hyaluronidase PH20; SC, subcutaneous.

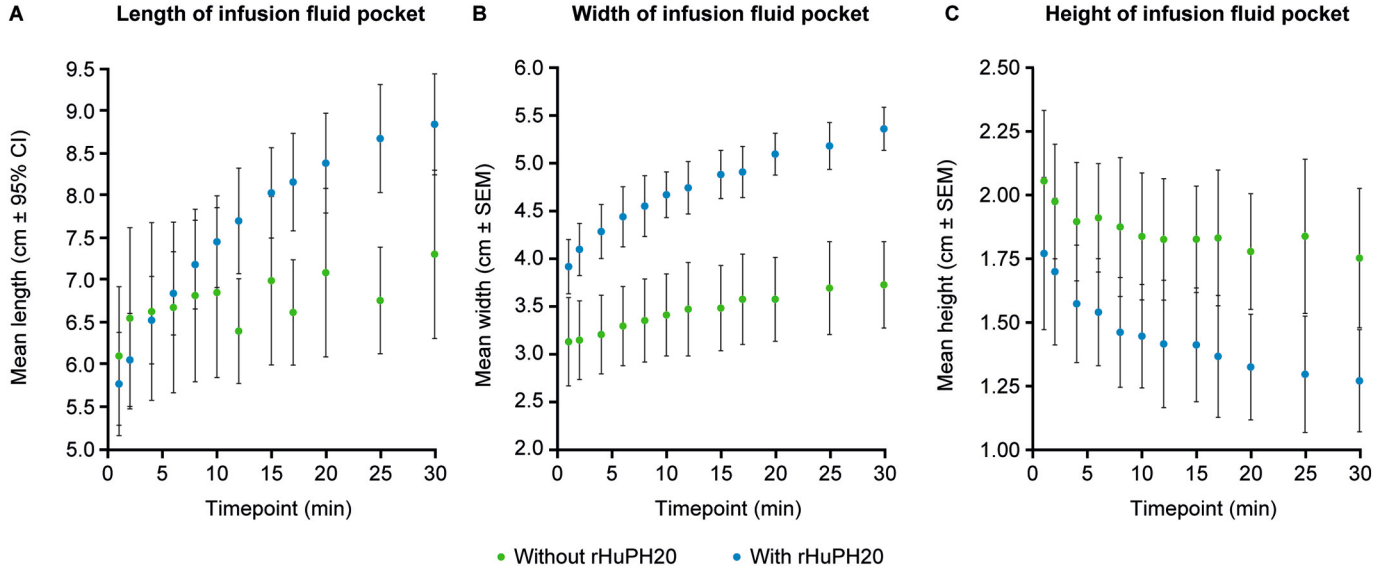

Fig. 5. Comparison of the average (A) length, (B) width, and (C) height of the fluid pockets of CA infusions (10 mL) from all flow rates with and without rHuPH20 over time post-infusion. The average (mean) across all animals ±95% CI are reported.
95% CI, 95% confidence interval; CA, contrast agent; rHuPH20, recombinant human hyaluronidase PH20.

3.5. 3D reconstruction of post-infusion time course for CA with and without rHuPH20

Dispersion of CA with rHuPH20 occurred rapidly, with an increase in fluid pocket volume occurring within the first 10 min after infusion and continuing throughout the entire post-infusion period (30 min; Fig. 7 and Supplemental online animation). The shapes of the CA fluid pockets with rHuPH20 administration were also significantly flatter than those of infusions of CA on its own, which only showed a very gradual increase in volume and minimal changes in height.

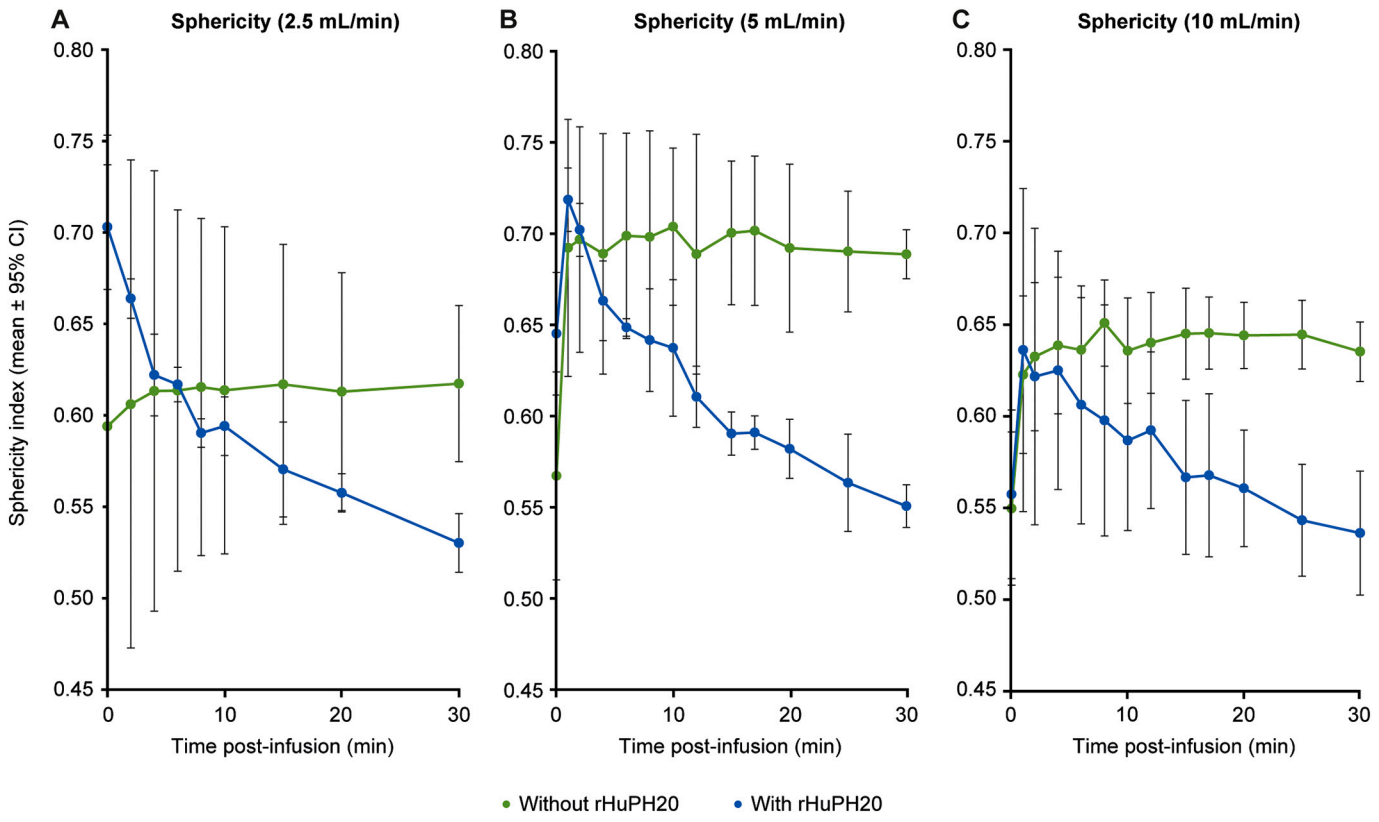

Fig. 6. Sphericity of post-infusion fluid pockets of CA with and without rHuPH20. Trendlines are based on a moving average with an interval of 2. The average (mean) across all animals ±95% CI are reported.
95% CI, 95% confidence interval; CA, contrast agent; rHuPH20, recombinant human hyaluronidase PH20.

4. Discussion

Although SC infusion is becoming a common route of administration for biotherapeutics (Bittner, Richter, & Schmidt, 2018), particularly if frequent treatments, long-term regimens, or self-administration are required, current knowledge about the dispersion of therapeutics in the SC space is limited. High-resolution imaging techniques that can provide real-time images have proven effective in studying drug permeation and diffusion in the SC space (Jockel, Roebrock, & Shergold, 2013; Kim, Park, & Lee, 2017; Thomsen et al., 2012). In the current study, using CT imaging, we were able to quantitatively measure the size, volume, and shape of the SC dispersion of a surrogate therapeutic fluid with and without rHuPH20 over time.

Using 3D imaging, we were able to demonstrate that, compared with administering CA alone, both the surface area and volume of rHuPH20-facilitated SC infusions of CA were significantly increased in the post-infusion SC space for all three infusion flow rates tested, confirming that rHuPH20 enhances the local dispersion of subcutaneously administered fluids. The increased dispersion of CA into the SC space occurs as the result of rHuPH20-mediated enzymatic degradation of HA. The observed increase in fluid pocket volumes beyond the administered 10 mL at time = 0 min, was likely a result of the decreasing density of CA as it spread through the SC space and an increase in space between CA molecules. Due to the thresholds used in the CT scans, minor changes in CA density could not be discriminated, only the outer edges of the fluid pocket.

The study also allowed for evaluation of the fluid pocket shape with and without rHuPH20. The fluid pockets for rHuPH20-facilitated infusions were flatter and wider than for infusions without rHuPH20, as a result of the greater decrease in the height of rHuPH20-facilitated infusions. This was accompanied by continual increases in the craniocaudal and lateromedial dimensions compared with infusions of CA alone. The decrease in sphericity observed in the rHuPH20-facilitated infusions compared with infusions of CA alone, mathematically describes this 3-dimensional dispersion pattern. Ultimately, the changes in the shape of the fluid pockets with rHuPH20 co-administration translate into reduced swelling around the infusion site.

In this study, the impact of infusion duration was controlled for by assessing three different infusion rates while maintaining the same total infusion volume of CA, either with or without rHuPH20. Following infusion with either rHuPH20 and CA or CA alone, all three infusion rates showed similar results for surface area, volume and sphericity of the post-infusion fluid pocket, demonstrating that rHuPH20 works to increase dispersion independent of the infusion rate.

The purpose of this study was to evaluate the value of CT imaging as a non-invasive method of assessing real-time spatial and temporal behavior of SC-administered fluids in the presence of rHuPH20. Through the use of CT, these results suggest that dispersion occurs via fluid flow in the SC space between the dermis and the muscle layer. The quantitative findings were supported by gross observations of the animals in this study. Infusions of CA combined with rHuPH20 resulted in either no visible swelling at the infusion sites, or mild swelling that was soft and only detectable by touch. Conversely, infusions of CA alone produced hard swelling that was easily visible. None of the animals showed intra-abdominal abnormalities after administration of rHuPH20-facilitated infusions or CA alone.

While conducted in an animal model, this study was designed to be translatable to the clinical setting. The selection of a contrast agent based on a macromolecule (iodixanol) with a high viscosity (12.7 cP) allowed it to be treated as surrogate of a therapeutic, as therapeutics are often formulated to high concentrations, and, consequently, high viscosity, to allow administration of smaller volumes (Tomar, Kumar, Singh, Goswami, & Li, 2016). In addition, the dose of rHuPH20 (2000 U/mL) evaluated in this study is consistent with the dose used in Food and

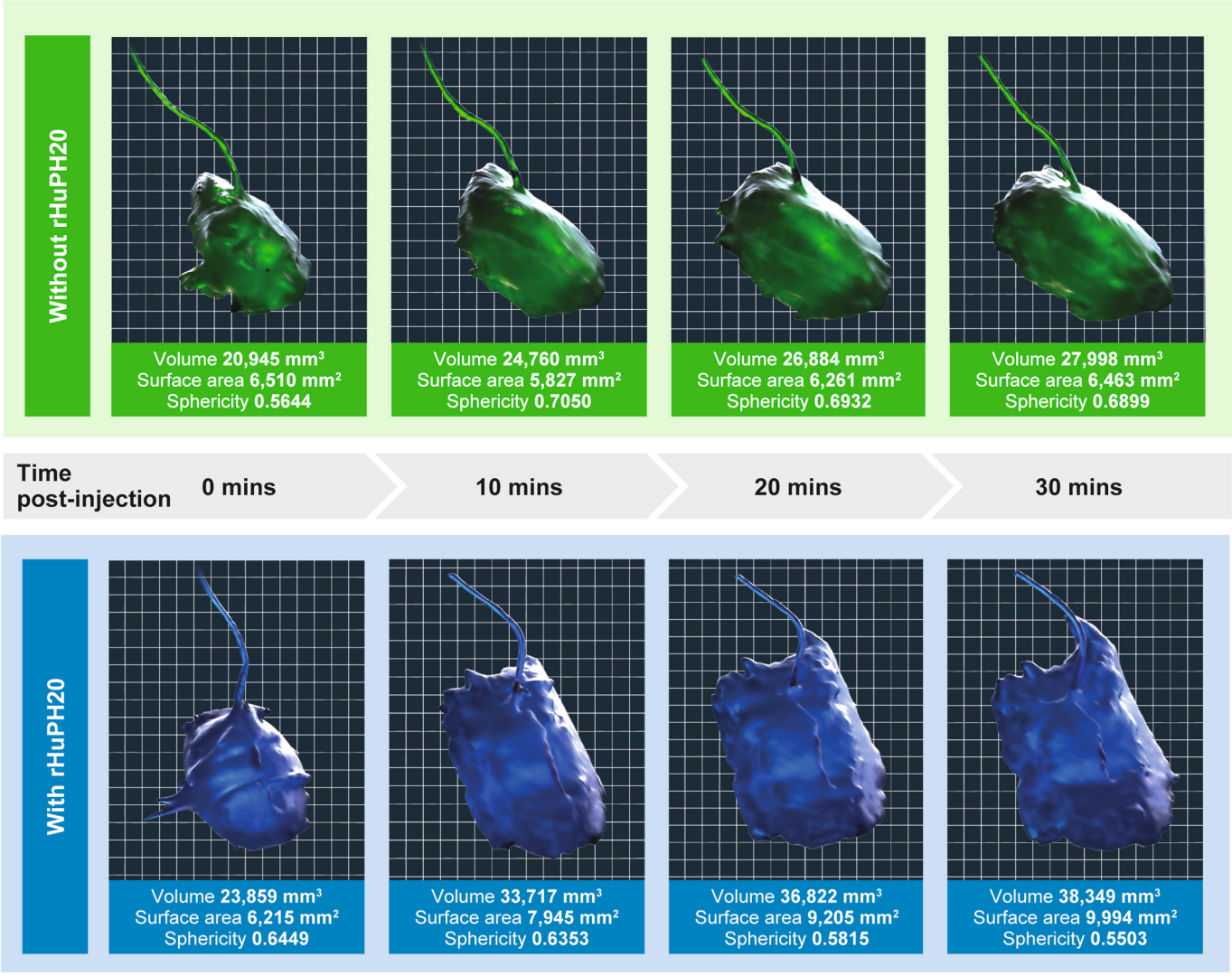

Fig. 7. Time course of post-infusion CA with and without rHuPH20 at an infusion rate of 5 mL/min.
CA, contrast agent; rHuPH20, recombinant human hyaluronidase PH20.

Drug Administration-approved therapeutics (e.g. RITUXAN HYCELA® and HERCEPTIN HYLECTA™) (Roche, 2017; Roche Products Ltd, 2019). Purpose-bred Yucatan miniature swine (*Sus scrofa domestica*) were chosen for their wide acceptance as the most appropriate non-human organism for modeling human skin anatomy, and their use has been validated in previous imaging and SC drug delivery studies (Jockel, Roebrock, & Shergold, 2013; Kang, Oh, Fu, Anderson, & Zepeda, 2013; Lunney, 2007). Furthermore, their size makes them well suited to imaging studies that may be challenging to conduct in small animal models, and allows the delivery of a clinically relevant volume of a therapeutic agent (Lunney, 2007). To reduce variation between animals, the animals in this exploratory study were sex, age and litter matched. A study sample size of 10 animals ($n = 3$–4 per group) was chosen to allow for the constraints of litter size and raising animals to young adolescence.

The quantification of the increased dispersion of a representative therapeutic fluid with rHuPH20 is potentially clinically relevant. As previous studies have demonstrated, by increasing the dispersion of SC infusions and decreasing the associated swelling, rHuPH20-facilitated drug delivery can enable larger volumes to be rapidly delivered subcutaneously with a lower risk of infusion site reactions and induration, potentially improving safety, comfort, and patient compliance for repeat infusions (Bookbinder et al., 2006; Thomas et al., 2009; Vaughn & Muchmore, 2011; Wasserman, 2012).

The study confirms the value of CT imaging as a non-invasive technique to assess the real-time spatial and temporal behavior of subcutaneously administered therapeutics. The techniques used here to quantify and model the dispersion of fluid in the SC space could be applied to assess the volumes, concentrations and administration rates of other new SC therapeutics, as well as the development of rHuPH20 co-formulations.

5. Conclusions

The results from this exploratory study provide a novel method of characterizing rapid fluid dispersion in the SC space with rHuPH20 using CT imaging. Using this technique, we showed that in comparison with CA alone, rHuPH20 significantly increased the post-infusion surface area and volume in the SC space for all flow rates. Administration of rHuPH20 with CA also resulted in a flatter, wider fluid pocket than infusion of CA without rHuPH20. In addition, the fluid pockets resulting from infusions of CA with rHuPH20 showed a continual decrease in sphericity over time, whereas the fluid pockets of CA without rHuPH20 showed no change in sphericity and remained relatively static. Together the results demonstrate how rHuPH20 can facilitate the SC administration of large volumes of a representative therapeutic fluid with

reduced swelling, compared with a representative therapeutic fluid administered alone, with dispersion likely occurring via fluid flow in the SC space between the dermis and the muscle layer. The study confirms the value of CT imaging to assess the dispersion of subcutaneously administered therapeutics and supports the use of the techniques in future studies.

Supplementary data to this article can be found online at https://doi.org/10.1016/j.vascn.2020.106936.

Author contributions

All authors were involved in the conception, design, analysis, and interpretation of the data, the drafting of the paper, and the final approval of the version to be published. All authors agree to be accountable for all aspects of the work.

Declaration of Competing Interest

The study was funded by Halozyme Therapeutics, Inc. RJC and DMT were formerly employees, owned stock, and had stock options in Halozyme Therapeutics, Inc. at the time of the study. MJL and DWK own stock and have stock options in Halozyme Therapeutics, Inc. KT is an employee of Altasciences Preclinical Seattle LLC and does not hold shares in the company.

Acknowledgments

The authors thank the dedicated staff at Altasciences Preclinical Seattle LLC (Everett, WA) for their skilled handling and care of the animals, and Dr. Seth Wallack (DVM, DACVR) for post-study CT analysis. Medical writing support, including assisting authors with the development of the outline and initial draft and incorporation of comments, was provided by Yanni Wang, PhD, Talya Underwood, MPhil, and William Stainsby, MSci; editorial support, including referencing, formatting, proofreading, and submission was provided by Michelle Seddon, Dip Psych, all of Paragon, Knutsford, UK, supported by Halozyme Therapeutics, Inc. Halozyme Therapeutics follows all current policies established by the International Committee of Medical Journal Editors and Good Publication Practice guidelines (https://www.ismpp.org/gpp3). The Sponsor was involved in the study design, collection, analysis, and interpretation of data, as well as data checking of information provided in the manuscript. However, ultimate responsibility for opinions, conclusions, and data interpretation lie with the authors.

The studies were conducted by SNBL USA Ltd. (Everett, WA) for Halozyme Therapeutics, Inc. and the data are held by the company. Additional information about the studies and/or datasets can be obtained by contacting Halozyme Therapeutics: 11388 Sorrento Valley Road, San Diego, CA 92121; Phone: +1 (858) 794-8889; Email: publications@halozyme.com.

References

Atkinson, W. S. (1949). Use of hyaluronidase with local anesthesia in ophthalmology: Preliminary report. *Archives of Ophthalmology, 42*(5), 628–633. https://doi.org/10.1001/archopht.1949.00900050638012.

Awwad, S., & Angkawinitwong, U. (2018). Overview of antibody drug delivery. *Pharmaceutics, 10*(3). https://doi.org/10.3390/pharmaceutics10030083.

Baumgartner, G., Gomar-Hoss, C., Sakr, L., Ulsperger, E., & Wogritsch, C. (1998). The impact of extracellular matrix on the chemoresistance of solid tumors–experimental and clinical results of hyaluronidase as additive to cytostatic chemotherapy. *Cancer Letters, 131*(1), 85–99. https://doi.org/10.1016/S0304-3835(98)00204-3.

Baxalta Innovation GmbH. (2018). Hyqvia (human normal immunoglobulin) summary of product characteristics. Retrieved from http://www.ema.europa.eu/docs/en_GB/document_library/EPAR_-_Product_Information/human/002491/WC500143851.pdf.

Biogen and Genentech USA Inc. (2017). Rituxan hycela (rituximab) prescribing information. Retrieved from https://www.gene.com/download/pdf/rituxan_hycela_prescribing.pdf.

Bittner, B., Richter, W. F., Hourcade-Potelleret, F., Herting, F., & Schmidt, J. (2014). Non-clinical pharmacokinetic/pharmacodynamic and early clinical studies supporting development of a novel subcutaneous formulation for the monoclonal antibody rituximab. *Drug Research (Stuttg), 64*(11), 569–575. https://doi.org/10.1055/s-0033-1363993.

Bittner, B., Richter, W., & Schmidt, J. (2018). Subcutaneous administration of biotherapeutics: An overview of current challenges and opportunities. *BioDrugs, 32*(5), 425–440. https://doi.org/10.1007/s40259-018-0295-0.

Bookbinder, L. H., Hofer, A., Haller, M. F., Zepeda, M. L., Keller, G. A., Lim, J. E., … Frost, G. I. (2006). A recombinant human enzyme for enhanced interstitial transport of therapeutics. *Journal of Controlled Release, 114*(2), 230–241. https://doi.org/10.1016/j.jconrel.2006.05.027.

De Cock, E., Pivot, X., Hauser, N., Verma, S., Kritikou, P., Millar, D., & Knoop, A. (2016). A time and motion study of subcutaneous versus intravenous trastuzumab in patients with her2-positive early breast cancer. *Cancer Medicine, 5*(3), 389–397. https://doi.org/10.1002/cam4.573.

Frost, G. I. (2007). Recombinant human hyaluronidase (rhuph20): An enabling platform for subcutaneous drug and fluid administration. *Expert Opinion on Drug Delivery, 4*(4), 427–440. https://doi.org/10.1517/17425247.4.4.427.

GE Healthcare Inc. (1996). Highlights of prescribing information: Visipaque. Retrieved from https://www.accessdata.fda.gov/drugsatfda_docs/label/2017/020808s026lbl.pdf.

Genentech Inc. (2020). Phesgo (pertuzumab, trastuzumab, and hyaluronidase-zzxf) injection, for subcutaneous use. Retrieved from https://www.gene.com/download/pdf/phesgo_prescribing.pdf.

Genmab. (2020). Genmab announces european marketing authorization for the subcutaneous formulation of darzalex® (daratumumab) for the treatment of patients with multiple myeloma. Retrieved from https://ir.genmab.com/news-releases/news-release-details/genmab-announces-european-marketing-authorization-subcutaneous/.

Halozyme Therapeutics Inc. (2016). Prescribing information hylenex recombinant (hyaluronidase human injection). Retrieved from http://hylenex.com/downloads/approved-uspi-lbl301feb2016.pdf.

Hunter, J. (2008). Subcutaneous injection technique. *Nursing Standard, 22*(21), 41–44. https://doi.org/10.7748/ns2008.01.22.21.41.c6418.

Jadin, L., Bookbinder, L. H., & Frost, G. I. (2012). A comprehensive model of hyaluronan turnover in the mouse. *Matrix Biology, 31*(2), 81–89. https://doi.org/10.1016/j.matbio.2011.11.002.

Janssen Biotech Inc. (2020). Highlights of prescribing information, darzalex faspro™ injection for subcutaneous use. Retrieved from https://www.accessdata.fda.gov/drugsatfda_docs/label/2020/761145s000lbl.pdf.

Jockel, J. P., Roebrock, P., & Shergold, O. A. (2013). Insulin depot formation in subcutaneoue tissue. *Journal of Diabetes Science and Technology, 7*(1), 227–237. https://doi.org/10.1177/193229681300700128.

Kang, D. W., Oh, D. A., Fu, G. Y., Anderson, J. M., & Zepeda, M. L. (2013). Porcine model to evaluate local tissue tolerability associated with subcutaneous delivery of protein. *Journal of Pharmacological and Toxicological Methods, 67*(3), 140–147. https://doi.org/10.1016/j.vascn.2013.01.011.

Kim, H., Park, H., & Lee, S. J. (2017). Effective method for drug injection into subcutaneous tissue. *Scientific Reports, 7*(1), 9613. https://doi.org/10.1038/s41598-017-10110-w.

Locke, K. W., Maneval, D. C., & LaBarre, M. J. (2019). Enhanze® drug delivery technology: A novel approach to subcutaneous administration using recombinant human hyaluronidase ph20. *Drug Delivery, 26*(1), 98–106. https://doi.org/10.1080/10717544.2018.1551442.

Lunney, J. K. (2007). Advances in swine biomedical model genomics. *International Journal of Biological Sciences, 3*(3), 179–184.

National Research Council. (2011). *Guide for the care and use of laboratory animals* (8th ed.). Washington, DC: The National Academies Press.

Pivot, X., Gligorov, J., Muller, V., Curigliano, G., Knoop, A., Verma, S., … PrefHer Study, G. (2014). Patients' preferences for subcutaneous trastuzumab versus conventional intravenous infusion for the adjuvant treatment of her2-positive early breast cancer: Final analysis of 488 patients in the international, randomized, two-cohort prefher study. *Annals of Oncology, 25*(10), 1979–1987. https://doi.org/10.1093/annonc/mdu364.

Richter, W. F., & Jacobsen, B. (2014). Subcutaneous absorption of biotherapeutics: Knowns and unknowns. *Drug Metabolism and Disposition, 42*(11), 1881–1889. https://doi.org/10.1124/dmd.114.059238.

Roche. (2017). Highlights of prescribing information: Rituxan hycela® (rituximab and hyaluronidase human) injection, for subcutaneous use. Retrieved from https://www.gene.com/medical-professionals/medicines/rituxan-hycela.

Roche Products Ltd. (2019). Prescribing information herceptin hylecta™ (trastuzumab and hyaluronidase-oysk) injection, for subcutaneous use. Retrieved from https://www.accessdata.fda.gov/drugsatfda_docs/label/2019/761106s000lbl.pdf.

Roche Registration GmbH. (2018a). Herceptin sc (trastuzumab) summary of product characteristics. Retrieved from http://www.ema.europa.eu/docs/en_GB/document_library/EPAR_-_Product_Information/human/000278/WC500074922.pdf.

Roche Registration GmbH. (2018b). Mabthera (rituximab) summary of product characteristics. Retrieved from http://www.ema.europa.eu/docs/en_GB/document_library/EPAR_-_Product_Information/human/000165/WC500025821.pdf.

Stern, R. (2003). Devising a pathway for hyaluronan catabolism: Are we there yet? *Glycobiology, 13*(12), 105R–115R. https://doi.org/10.1093/glycob/cwg112%JGlycobiology.

Takeda Pharmaceuticals. (2014). Prescribing information hyqvia [immune globulin infusion 10% (human) with recombinant human hyaluronidase]. Retrieved from https://www.fda.gov/downloads/ApprovedProducts/UCM414440.pdf.

Thomas, J. R., Wallace, M. S., Yocum, R. C., Vaughn, D. E., Haller, M. F., & Flament, J. (2009). The infuse-morphine study: Use of recombinant human hyaluronidase (rhuph20) to enhance the absorption of subcutaneously administered morphine in patients with advanced illness. *Journal of Pain and Symptom Management, 38*(5), 663–672. https://doi.org/10.1016/j.jpainsymman.2009.03.009.

Thomsen, M., Poulsen, M., Bech, M., Velroyen, A., Herzen, J., Beckmann, F., … Pfeiffer, F. (2012). Visualization of subcutaneous insulin injections by x-ray computed tomography. *Physics in Medicine and Biology, 57*(21), 7191–7203. https://doi.org/10.1088/0031-9155/57/21/7191.

Tomar, D. S., Kumar, S., Singh, S. K., Goswami, S., & Li, L. (2016). Molecular basis of high viscosity in concentrated antibody solutions: Strategies for high concentration drug product development. *MAbs, 8*(2), 216–228. https://doi.org/10.1080/19420862.2015.1128606.

Vaughn, D. E., & Muchmore, D. B. (2011). Use of recombinant human hyaluronidase to accelerate rapid insulin analogue absorption: Experience with subcutaneous injection and continuous infusion. *Endocrine Practice, 17*(6), 914–921. https://doi.org/10.4158/EP11297.RA.

Vigetti, D., Viola, M., Karousou, E., De Luca, G., & Passi, A. (2014). Metabolic control of hyaluronan synthases. *Matrix Biology, 35*, 8–13. https://doi.org/10.1016/j.matbio.2013.10.002.

Wadell, H. (1935). Volume, shape, and roundness of quartz particles. *The Journal of Geology, 43*(3), 250–280. https://doi.org/10.1086/624298.

Wasserman, R. L. (2012). Progress in gammaglobulin therapy for immunodeficiency: From subcutaneous to intravenous infusions and back again. *Journal of Clinical Immunology, 32*(6), 1153–1164. https://doi.org/10.1007/s10875-012-9740-x.

Watson, D. (1993). Hyaluronidase. *British Journal of Anaesthesia, 71*(3), 422–425.

Williams, E. L., & Edwards, C. J. (2006). Patient preferences in choosing anti-tnf therapies-r1. *Rheumatology (Oxford), 45*(12), 1575–1576. https://doi.org/10.1093/rheumatology/kel369.

Wynne, C., Harvey, V., Schwabe, C., Waaka, D., McIntyre, C., & Bittner, B. (2013). Comparison of subcutaneous and intravenous administration of trastuzumab: A phase i/ib trial in healthy male volunteers and patients with her2-positive breast cancer. *Journal of Clinical Pharmacology, 53*(2), 192–201. https://doi.org/10.1177/0091270012436560.

Yocum, R. C., Kennard, D., & Heiner, L. S. (2007). Assessment and implication of the allergic sensitivity to a single dose of recombinant human hyaluronidase injection: A double-blind, placebo-controlled clinical trial. *Journal of Infusion Nursing, 30*(5), 293–299. https://doi.org/10.1097/01.NAN.0000292572.70387.17.